



## Carbon use efficiency of terrestrial ecosystems in desert/grassland biome transition zone: A case in Ningxia province, northwest China

Lingtong Du<sup>a,b,c,\*</sup>, Fei Gong<sup>a,b</sup>, Yijian Zeng<sup>c</sup>, Longlong Ma<sup>a,b</sup>, Chenglong Qiao<sup>a,b</sup>, Hongyue Wu<sup>a,b</sup>

<sup>a</sup> Breeding Base for State Key Laboratory of Land Degradation and Ecological Restoration in Northwest China, Ningxia University, Yinchuan 750021, China

<sup>b</sup> Key Laboratory for Restoration and Reconstruction of Degraded Ecosystem in Northwest China of Ministry of Education, Ningxia University, Yinchuan 750021, China

<sup>c</sup> Faculty of Geo-Information Science and Earth Observation, University of Twente, 7500 AE Enschede, Netherlands

### ARTICLE INFO

#### Keywords:

Carbon use efficiency (CUE)  
Terrestrial ecosystem  
Net primary productivity (NPP)  
Desert/grassland biome transition zone  
Arid and semi-arid region  
MODIS

### ABSTRACT

Terrestrial ecosystems play a critical role in the global carbon cycle and the feedbacks of carbon cycle will significantly impact future climate change. It's worth noting that semi-arid biomes in the Southern Hemisphere have driven the global carbon sink anomaly over the past 30 years. However, how does the desert/grassland biome transition zone, a part of arid and semi-arid biomes, respond to climate change and anthropogenic activities in carbon use efficiency (CUE) is still unclear. Therefore, based on the CUE of terrestrial ecosystem estimated by the moderate resolution imaging spectroradiometer (MODIS) data from 2001 to 2017, the spatial and temporal characteristics of CUE in Ningxia province, a typical desert/grassland biome transition zone, were studied. The main driving factors in climate and ecosystem were also investigated by partial correlation analysis. Results showed that the CUE of terrestrial ecosystems in desert/grassland biome transition zone is higher than 0.5, a constant value of CUE defined in many ecological models. However, the CUE varies with the ecosystem types even when they are located in the same climatic zone. There is a decreasing trend of annual CUE in the period of 2001–2017 and most of them will persistently decrease in future at pixels scales, which could be mainly caused by the land use change. Comparing the habitat conditions, we found the lower canopy density and water stress could increase the CUE in the same ecosystem, which indicates the plant could increase their efficiency of transforming carbon from the atmosphere to terrestrial biomass in adverse environment. Finally, the CUE significantly correlated to net primary productivity (NPP) and autotrophic respiration ( $R_a$ ) in ecosystem processes, meanwhile water stress (lower precipitation) and heat stress (higher temperature) could increase the CUE, but the temperature has variable impacts in different ecosystem.

### 1. Introduction

Global carbon cycle is one of the issues mostly discussed worldwide (Falkowski et al., 2000; Fang et al., 2018). Terrestrial ecosystems play a critical role in the global carbon cycle and the feedbacks of carbon cycle will significantly impact future climate change (Schimel et al., 2015; Schimel, 1995). Ecosystem carbon is mainly fixed by photosynthesis, and one third of the carbon in the atmosphere is fixed by the terrestrial ecosystem (Schimel, 1995). However, the carbon capture ability is different in each terrestrial ecosystem. Forests and grasslands are two important parts of terrestrial ecosystem and account for 51% of the global terrestrial ecosystem (31% of forests and 20% of grassland), at least 10%–30% of global soil carbon is stocked in grassland ecosystem

(Scurlock and Hall, 1998). The human induced land use change, such as forestation, deforestation and grazing, would have a unexpectedly impact on global carbon stocks but it remains poorly quantified (Chen et al., 2019; Erb et al., 2018; Lu et al., 2018). The recent report shows that there is a great potential in global tree restoration, which could increase an extra 0.9 billion hectares of canopy cover and store an additional 205 gigatonnes of carbon (Bastin et al., 2019). Meanwhile, the grassland ecosystem is sensitive to climate change and it would alter the carbon storage frequently (Fay et al., 2008; Rodionov et al., 2010). A simulation based on terrestrial biogeochemical model shown that the global carbon sink anomaly was driven by semi-arid biomes in the Southern Hemisphere, which is an important driver of global carbon cycle inter-annual variability (Poulter et al., 2014). Desert/grassland

\* Corresponding author at: No. 489 Hanlanshan Road, Yinchuan 750021, PR China.

E-mail address: [dult80@nxu.edu.cn](mailto:dult80@nxu.edu.cn) (L. Du).

<https://doi.org/10.1016/j.ecolind.2020.106971>

Received 17 March 2020; Received in revised form 10 August 2020; Accepted 15 September 2020

Available online 25 September 2020

1470-160X/© 2020 The Authors.

Published by Elsevier Ltd.

This is an open access article under the CC BY-NC-ND license

(<http://creativecommons.org/licenses/by-nc-nd/4.0/>).

biome transition zone between the desert and grassland is characterized by arid and semi-arid climate and distributed around the world widely (Hou et al., 2019). A shift in the status of vegetation growth and phenology in desert/grassland biome transition zone under the context of global climate change could affect the carbon cycle of terrestrial ecosystems. Nevertheless, the carbon cycle of terrestrial ecosystems in desert/grassland biome transition zone has been seldomly studied, especially on its responses to climate change and anthropogenic activities.

Carbon use efficiency (CUE) of terrestrial ecosystem is defined as the ratio of net primary productivity (NPP) to gross primary productivity (GPP) (Chambers et al., 2004; Curtis et al., 2005), as a key measure of carbon transformation, and describes the capacity of ecosystem to transfer carbon from the atmosphere to terrestrial biomass (Delucia et al., 2007). The NPP/GPP ratio had been hypothesized as universal across biomes, tree species and stand ages (Waring et al., 1998). A constant CUE of 0.5 has been widely used in terrestrial carbon cycle models, such as the Carnegie-Ames-Stanford-Approach (CASA) model, or the Marine Biological Laboratory/Soil Plant-Atmosphere Canopy Model, for regional or global modeling purposes (Delucia et al., 2007). The previous studies confirmed that the autotrophic respiration ( $R_a$ ) was dependent on GPP but there is a nonlinear response of the  $R_a$  to GPP ratio to temperature variations (Piao et al., 2010). Nonetheless, the hypothesis of constant CUE is not valid, as the value of this ratio is not constant and always is influenced by environmental factors, stand developments, managements and ecosystem types (Choudhury, 2000; Collalti and Prentice, 2019; Ogawa, 2011). CUE was even regarded as a flexible and scale-dependent index from individuals to ecosystems (Manzoni et al., 2018). A literature survey integrated a large number of estimated CUE about forests used biomass method and modeling method from 1975 to 2005 and concluded that the CUE of different types of forest were between 0.20 and 0.83 (Delucia et al., 2007). It has been also mentioned that CUE is quite sensitive to climate and growing stage (Dillaway and Kruger, 2014). Same as the water use efficiency (WUE), the ratio of water loss to carbon gain, CUE is a key characteristic of ecosystem function that is central to the global cycles of carbon (Keenan et al., 2013). However, the characteristics and variation of CUE with different ecosystems and at varying seasonal and annual scales are still not clearly studied.

The determination of CUE in different ecosystems is actually to determine the components of GPP that includes its net photosynthetic carbon fixation (NPP) and autotrophic respiration ( $R_a$ ) (Choudhury, 2000). At site scale, the measurement of productivity is mainly based on traditional biometric method, which is to measure the above-ground and underground biomass of plants during different periods and establish an allometric equation of biomass to estimate the NPP of the ecosystem (Chambers et al., 2004). The net carbon flux between ecosystem and atmosphere can be measured with the eddy covariance technique, a micrometeorological technology (Baldocchi et al., 1988), which is, however, limited by its measurement footprint being local. On the other hand, the remote sensing has the advantage to observe the spatial and temporal changes of ecosystem CUE at regional or even global scale (He et al., 2018; Letchov, 2018). Based on moderate resolution imaging spectroradiometer (MODIS) data from 2000 to 2003, the global scale terrestrial ecosystem CUE was observed and the effects of ecosystem type, geographical location and climate on the pattern of NPP to GPP ratio were discussed (Zhang et al., 2009). The spatial variations of CUE from MODIS satellite data and process-based models shows that the mechanisms behind spatiotemporal changes in  $R_a$  is a critical step towards better quantifying global CUE (He et al., 2018). Furthermore, the CUE is proven to be significantly related to forest type, and climatic and geographic factors, being variable rather than constant (Kwon and Larsen, 2013).

Grassland is one of big ecosystems and plays a significant role in the carbon cycle (Hou et al., 2018). A grassland carbon use efficiency from global scale was monitored by remote sensing and it was found the CUE

of grassland had considerable spatial variation associated with grassland types, geographical locations and climate changes (Yang et al., 2017). Moreover, the CUE of the grassland had significant correlations with the drought severity index (DSI), and the drought could induce dynamics of CUE in grassland ecosystem (Gang et al., 2016). Nevertheless, the CUE of desert/grassland biome transition zone is still not well studied, although the vegetation of this zone could be affected seriously by climate change and anthropogenic activities (Hou et al., 2019).

Ningxia Hui Autonomous Region (Ningxia province) in northwest of China, a typical desert/grassland biome transition zone with rich ecosystem types, has implemented vegetation reconstruction in the past three decades. It is an ideal transect sample for studying the CUE of terrestrial ecosystems in desert/grassland biome transition zone. Revegetation of degraded ecosystems was popular in northwest of China and it provides a significant ecological benefits (Feng et al., 2016). Besides providing opportunities for carbon sequestration (Feng et al., 2016), it can also change the CUE of ecosystem. Therefore, the objectives of this study are to calculate and compare the spatiotemporal pattern of CUEs of varied ecosystems at a desert/grassland biome transition zone, using GPP and NPP products of MODIS. The driving factors of CUE variation will be analyzed with partial correlation analysis methods. The results of this study can help us to understand the CUE of terrestrial ecosystem in the desert/grassland biome transition zone under the background of climate change and anthropogenic activities, and provide a theoretical basis for regional economic development and ecological environment protection.

## 2. Materials and methods

### 2.1. Study area

As one of the smallest provinces in China, Ningxia province is located from N35°14' to N39°23' and from E104°17' to E107°39' with the reference frame of WGS84, has a total area of  $5.18 \times 10^6$  km<sup>2</sup>. In administrative division, Ningxia is divided in five prefecture cities that are Shizuishan, Yinchuan, Wuzhong, Zhongwei, and Guyuan (Du et al., 2017). Meanwhile, the province can be divided into three ecological zones with the geographical location stretching from the Helen Mountains in the north to the Liupan Mountains on the Loess Plateau in the south (Fig. 1). The Yellow River flows through the northern part of Ningxia and forms a fertile alluvial plain, where irrigation channels had been built on a 400 km stretch of the river in the Qin and Han dynasties. The northern part of Ningxia belongs to the arid climate but has abundant water resources which induced there an irrigated oasis landscape. The middle part of Ningxia is a farming-pastoral transition zone dominated by vast desert steppe and partial rain-fed agriculture with semi-arid climate. It is also a desert/grassland biome transition zone since there had been serious desertification and consequently a forcefully implemented conservation (Ho, 2000; Wang et al., 2014). Hence, the natural ecology and environment in arid zone of middle Ningxia is fragile. Southern Ningxia is part of the Chinese Loess Plateau, which is famous for its intensive soil erosion due to the specific geographic landscape, soil and climatic conditions, and long history of anthropogenic activities. The climatic characteristics of different geographical divisions in Ningxia province are quite different. The annual average temperature is 5–9 °C, and the annual precipitation varies from 200 to 700 mm between the northern plain and the southern mountainous region. The annual potential evapotranspiration is approximately 2000 mm, which is much higher than precipitation (Ghulam et al., 2007).

Ningxia province has typical characteristics of ecosystem transition from desert to grassland (Hou et al., 2019). The grassland ecosystem is widely distributed in the arid zone of middle Ningxia, the foothills of Helan Mountain and the loess hilly area of southern Ningxia. The area of grassland is about  $2.25 \times 10^6$  km<sup>2</sup>, accounting for 43.44% of the whole province, which is the most abundantly distributed terrestrial ecosystem in Ningxia. The farmland ecosystem is mainly distributed in the Yellow

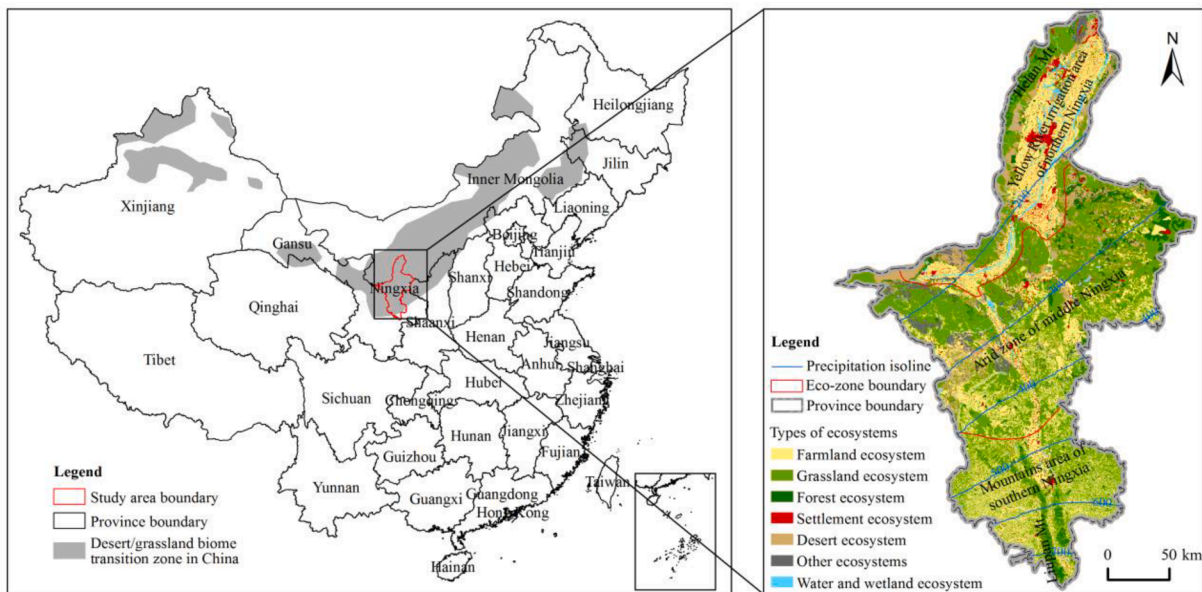


Fig. 1. Location of study area and terrestrial ecosystems of Ningxia. Note: desert/grassland biome transition zone was derived from Hou et al. (2019).

River plain of northern Ningxia with irrigated agriculture and the hilly and mountains area of middle-southern Ningxia with rain-fed agriculture. The area of farmland is about  $1.67 \times 10^6$   $\text{hm}^2$ , accounting for 32.24% of whole province. Forest ecosystem is distributed in the Helan Mountain and Liupan Mountain area, which is about  $0.34 \times 10^6$   $\text{hm}^2$  and accounting for 6.56% of the whole province (Fig. 1).

## 2.2. MODIS GPP, NPP data and CUE calculation

GPP is defined as the amount of energy and carbon captured and stored as biomass by the ecosystem (mainly by green plants) per unit of time through photosynthesis. GPP represents the initial material and energy entering the terrestrial ecosystem. The MODIS GPP product (MOD17A2H) is a cumulative 8-day composite of values with 500 m (m) pixel size and provides continuous estimates of GPP across Earth's entire vegetated land surface. The product was based on the radiation use efficiency concept that converts the absorbed photosynthetically active radiation (APAR) via a conversion efficiency parameter,  $\epsilon$ , which varies by vegetation types and climate conditions, to productivity of ecosystem (Running et al., 2004). Such GPP product is useful for global carbon cycle analysis, ecosystem status assessment, and environmental change monitoring (Zhao and Running, 2010). Here, the MODIS GPP product (version 6) datasets that covered Ningxia province over the period of 2001–2017 (tile h27v5) were collected from the United States Geological Survey (USGS) website (<https://e4ftl01.cr.usgs.gov>). The data were re-projected from a sinusoidal to an Albers conical equal area projection, using a bilinear re-sampling operator in MODIS reprojection tool (MRT). The 8-day composite of GPP values were used to synthesize monthly GPP datasets with the Interactive Data Language (IDL) software by a simple accumulation algorithm that the monthly values of GPP were calculated weighting with the number of days belonging to each month based on 8-day GPP (Du et al., 2013). Then, the annual GPP datasets were calculated by the same algorithm.

NPP, the amount of biomass created by plants that is usable to the rest of the food chain, is calculated by GPP subtracting  $R_a$ . NPP reflects the efficiency of plant fixation and transformation of photosynthate, and also determines the materials and energy available for heterotrophic organisms (herbivores and humans). The  $R_a$  of plant can be divided into the maintenance respiration ( $R_m$ ) and the growth respiration ( $R_g$ ) based on the algorithm of MOD17A2. Because the official NPP products are at annual interval, the monthly NPP was calculated by the 8-day net photosynthesis

( $PSN_{net}$ ) that is released together with the 8-day GPP in the same dataset. The algorithm of MOD17A2 is as follows (Running and Zhao, 2015).

$$NPP = GPP - R_a \quad (1)$$

$$R_a = R_m + R_g \quad (2)$$

$$PSN_{net} = GPP - R_m \quad (3)$$

$$NPP = PSN_{net} - R_g \quad (4)$$

$R_g$  is the energy cost for constructing organic compounds fixed by photosynthesis, which is defined as a function of annual maximum leaf area index (LAI) in previous algorithm. In the collection 6 of MOD17A2, the algorithm for growth respiration was updated by empirically parameterizing  $R_g$  as 25% of NPP (Running and Zhao, 2015). Therefore, NPP could be directly calculated by  $PSN_{net}$ .

$$R_g = 0.25 * NPP \quad (5)$$

$$NPP = 0.8 * PSN_{net} \quad (6)$$

The CUE not only represents the capacity of plants in converting assimilated atmospheric carbon dioxide to ecosystem carbon storage, but also the effect of autotrophic respiration consumption on vegetation productivity. CUE is an important indicator to compare the differences of carbon cycle in different ecosystems. Based on the GPP and NPP datasets, the CUE at pixel scale was calculated as:

$$CUE = \frac{NPP}{GPP} \quad (7)$$

There are a number of studies over various ecosystems worldwide to evaluate the performance of MODIS GPP/NPP that derived by different collections of algorithm (Gebremichael and Barros, 2006; Sjöström et al., 2013) and explore the potential of algorithm improvement (Sjöström et al., 2011, 2009). The results have helped to increase the confidence of MODIS GPP/NPP products application worldwide and the appropriate accuracy of MODIS GPP/NPP in most ecosystems provides a basis for calculating a high precise CUE in this research.

## 2.3. Ecosystem classification data and meteorological data

The original land use data of the study area from 2010 (1:100000 scale) was used to produce an ecosystem classification dataset. The land

use dataset was provided by the Cold and Arid Regions Science Data Center at Lanzhou (<http://westdc.westgis.ac.cn>) and it interpreted from Landsat-TM/ETM images with 30 m resolution. As a land use dataset sharing for public, its overall accuracy was higher than 95% in the first level categories (Tian et al., 2014). The multiple complex ecosystems of Ningxia province can be divided into 7 categories that include farmland ecosystem, grassland ecosystem, forest ecosystem, water and wetland ecosystem, desert ecosystem, settlement ecosystem and other ecosystem using an ecosystem classification system based on remote sensing technology in China (Ouyang et al., 2015).

Climate data (temperature and precipitation) from 2001 to 2017 were obtained from the China Meteorological Data Sharing Service System of the China Meteorological Administration (<http://cdc.cma.gov.cn/>). A total of 14 stations, including all stations of Ningxia (10 stations) and parts of stations of Shaanxi, Gansu and Inner Mongolia, were selected to interpolate spatial climate datasets using the Australian National University Spline (ANUSPLIN) method, and the result of the study area was projected and transformed to synthesize continuous raster data.

#### 2.4. Linear regression trend analysis

Linear regression is a statistical procedure for calculating the value of a dependent variable from an independent variable. Here, the years when the CUE data were collected are assumed as an independent variable, the linear regression method of ordinary least squares (OLS) was used to detect the trend of time series CUE at annual temporal scale. The slope of the regression equation ( $k$ ) is a best indicator for studying the trend of the CUE and it was calculated at pixel scale in IDL software. Then, an  $F$  test was used to check the significance level of the linear regression model. The formulation is as follows:

$$k = \frac{n \times \sum_{i=1}^n i \times CUE_i - \sum_{i=1}^n i \times \sum_{i=1}^n CUE_i}{n \times \sum_{i=1}^n i^2 - (\sum_{i=1}^n i)^2} \quad (8)$$

where  $k$  is the slope of the regression equation;  $n$  is the length of study period, here  $n = 17$  as the study period from 2001 to 2017;  $i$  is numerical order of years and 1 for year 2000, 2 for year 2001, ... $n$ ;  $CUE_i$  is the value of annual CUE in year  $i$ . If  $k$  in Eq. (8) is positive, it indicates the CUE has an increasing trend, and vice versa. Based on the slopes and the results of  $F$  test ( $P = 0.05$ ), there are four types of CUE change were obtained, as significant increasing, non-significant increasing, non-significant decreasing and significant decreasing.

#### 2.5. Rescaled range analysis

It is a fact that long-term persistence is present in several natural and human-associated processes, and the rescaled range analysis are widely used to detect time series of natural observation data for characteristics of long-term persistence (Araujo and Celeste, 2019). Here, the rescaled range analysis was used to check if the CUE time series from 2001 to 2017 for a persistence trend in future. The principle and formulation of rescaled range analysis are as follows (Araujo and Celeste, 2019):

Given an observed time series of variables  $\xi(t)$ ,  $t = 1, 2, \dots, n$ , for any moment  $\tau \geq 1$ , several designed sequences are:

$$\text{mean} : \langle \xi \rangle_\tau = \frac{1}{\tau} \sum_{t=1}^{\tau} \xi(t) \quad \tau = 1, 2, \dots, n \quad (9)$$

$$\text{Cumulative deviation} : X(t, \tau) = \sum_{u=1}^{\tau} (\xi(u) - \langle \xi \rangle_\tau) \quad 1 \leq t \leq \tau \quad (10)$$

$$\text{Range} : R(\tau) = X(t, \tau)_{\max} - X(t, \tau)_{\min} \quad \tau = 1, 2, \dots \quad (11)$$

$$\text{Standard deviation} : S(\tau) = \sqrt{\frac{1}{\tau} \sum_{t=1}^{\tau} (\xi(t) - \langle \xi \rangle_\tau)^2} \quad \tau = 1, 2, \dots \quad (12)$$

$$\text{Then, the rescaled adjusted range was defined as : } R/S = \frac{R(\tau)}{S(\tau)} \quad (13)$$

When  $R/S \propto \tau^H$ , it indicates the natural stochastic series has the Hurst phenomenon and  $H$  is called Hurst exponent. When  $0.5 < H < 1$ , it indicates that the series of variables possesses a long-term persistence feature, and their future trend is consistent with the past. When  $H = 0.5$ , it indicates that the series of variables is a random sequence. When  $0 < H < 0.5$ , it indicates that the series of variables has an anti-persistence feature and their future trend will be the opposite to the past.

#### 2.6. Partial correlation analysis

In probability theory and statistics, partial correlation measures the degree of association between two random variables, with the effect of the controlling random variables removed (Baba et al., 2004). In order find the driving factors of CUE change, a partial correlation analysis was performed, because many factors are not independent and have a self-correlation with the change of season and phenology of plant. Afterwards, the scatters were plotted using partial correlation that was suggested in ecological studies (Moya-Laraño and Corcobado, 2008). The partial correlation coefficient is calculated as follows (Li et al., 2013):

$$r_{xy.z} = \frac{r_{xy} - r_{xz}r_{yz}}{\sqrt{(1 - r_{xz}^2)(1 - r_{yz}^2)}} \quad (14)$$

where  $r_{xy.z}$  is the partial correlation coefficient between variables  $x$  and  $y$  for fixed variable  $z$ ;  $r_{xy}$ ,  $r_{xz}$  and  $r_{yz}$  is respectively the correlation coefficient between variables  $x$  and  $y$ ,  $x$  and  $z$  and  $y$  and  $z$ . The  $t$  test was used to check the significance of partial correlation coefficients.

### 3. Results and data analysis

#### 3.1. Spatial patterns of CUE

Fig. 2 shown the spatial patterns of annual CUE from 2001 and 2017, and the average CUE of whole Ningxia province is 0.59, ranging from 0.36 to 0.69 with standard deviation of 0.05, higher than the CUE of 0.5 defined in many ecological models. The obvious characteristic was that CUEs are heterogeneous in different geographical area with various terrestrial ecosystems types. From the view of geographic spatial properties, the highest CUE mainly occur in southeastern part of the arid zone of middle Ningxia with precipitation between 250 mm and 350 mm, and mountainous area of southern Ningxia, except Liupan Mountain. These areas were mainly farmland ecosystem with dry cropland in mountainous or hill areas and grassland ecosystem with low or medium coverage. In contrast, the lowest CUE is distributed in irrigation area of northern Ningxia along the valley of the Yellow River and its branches, and in the mountains including Helan Mt. in north and Liupan Mt. in south. More than half of the arid zone of middle Ningxia, which was desert steppe in grassland ecosystem, has medium CUE ranging from 0.58 to 0.61. The spatial patterns of annual CUE are obviously coupled with the distribution of ecosystem in Ningxia province but the CUE varies with the ecosystem types even when they are located in same climatic zone (Fig. 2).

#### 3.2. CUE of different ecosystems

The annual CUE data from 2001 to 2017 was masked by seven ecosystem types using spatial overlay analysis methods and the statistics of CUE of each ecosystem was showed in Fig. 3a. The CUE of these seven ecosystem types in Ningxia ranged from 0.57 to 0.63. The highest one is grassland ecosystem, the largest ecosystem in Ningxia province, with the CUE of 0.63 but with a narrow variation range. The next is forest ecosystem that has CUE of 0.60 also with a limited range. In contrast, the water and wetland ecosystem has the lowest CUE of 0.57 but with larger

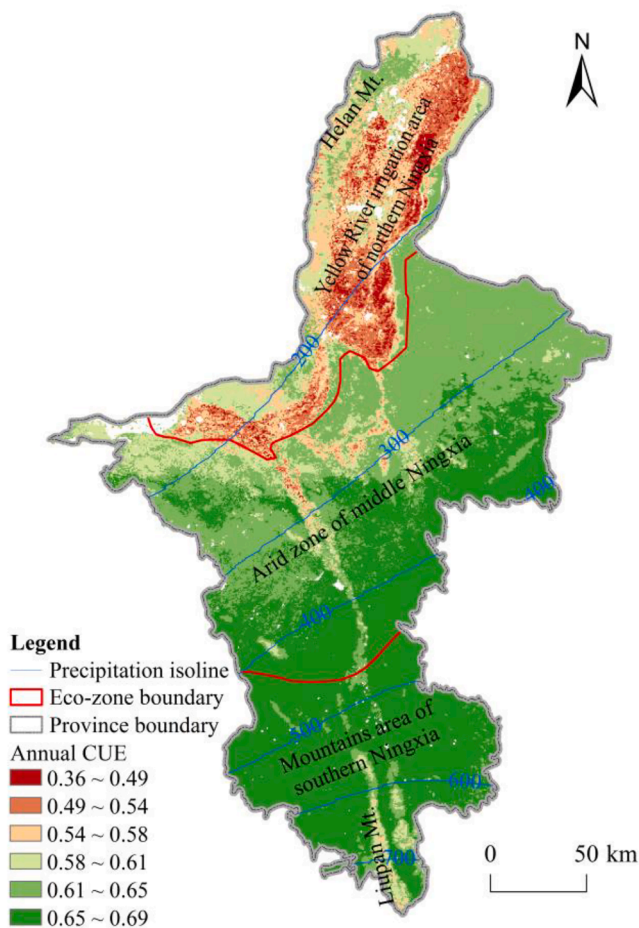


Fig. 2. Spatial characteristics of average annual CUE from 2001 to 2017.

variations, while its area only accounts for 2.14% of the whole Ningxia province. The CUE of farmland ecosystem, the second largest ecosystem in Ningxia province, has median value of all ecosystems. The CUE of settlement ecosystem, desert ecosystem and other ecosystem are 0.58, 0.59 and 0.60, respectively, but their areas only account for <10% of the whole Ningxia province.

The grassland ecosystem has the strongest capacity to transfer carbon from atmosphere to terrestrial biomass for its highest CUE although its cumulative biomass is lower. One of the reasons is that grassland has lower autotrophic respiration consumption and accumulates higher NPP than other ecosystems with the same GPP. The farmland ecosystem and forest ecosystem also have higher photosynthetic carbon fixation

capacity. Furthermore, the farmland has large area and forest has high cumulative biomass, which make them the main carbon storage in Ningxia province. In the following, the characteristics of CUE, based on the next level classification of land use types, in each ecosystem of farmland, grassland and forest were discussed. The farmland ecosystem includes the paddy field, irrigated cropland in plain, dry croplands in the mountains and hill areas, since they have various cultivations and geographic conditions. According to the canopy coverage, the grassland ecosystem can be divided into high, medium and low coverage grassland. The forest ecosystem also has four classes that are forest land, woodland, shrub land and sparsely woodland. The CUE of each land use types in three ecosystems are shown in Fig. 3b.

The paddy field had the lowest CUE with the largest variation range among farmland which is distributed in the Yellow River irrigation area of northern Ningxia, and accounts for 10.33% of the whole province (Fig. 2). The dry cropland on the hills and mountains are mainly distributed in the middle southern and southern of Ningxia and they had higher CUE than paddy field and irrigated cropland in plain. The CUE of land use types in farmland ecosystem had the same sequence with their intensity of water stress. In general, the sequence of water stress from high to low is dry cropland on mountain, dry cropland on hill, irrigated cropland on plain and paddy field, which is same with the magnitude sequence of CUE and that derives the stronger water stress in farmland led to higher CUE. In the grassland ecosystem, the similar pattern as in farmland was found that the lower coverage with the higher CUE, which is also related with the water supply of grassland ecosystem. The low coverage grasslands with the highest CUE, account for 21.53% of the whole province, are mainly the desert steppe and are distributed in the arid zone of middle Ningxia, where precipitation is between 200 and 400 mm. However, the grassland with medium and high coverage, which usually increased with the rising of precipitation gradient, had lower CUE. The land use types of forest ecosystem also show that the lower canopy density with the higher CUE. The CUE in order from low to high is for forest land, woodland, shrub land and sparse woodland correspondingly.

### 3.3. Characteristics of monthly and annual CUE

The monthly CUE within a year in the whole Ningxia province showed that there were two peaks in April and October separately with the values of 0.68 and 0.67, respectively (Fig. 4a). The curve of CUE in a year follows the plant phenology in Ningxia province. With the plants activity recovering, leaf and stem biomass grew rapidly in spring (March to May) and more photosynthesis was used for NPP growth accumulation. However, the CUE began to decrease in summer (June to August) and stayed at low level; the minimum of CUE in summer was 0.57 and reached in July. This phenomenon was caused by the strong autotrophic respiration consumption of plants in summer, which leads to slow accumulation of NPP with the same photosynthetic intensity. Such

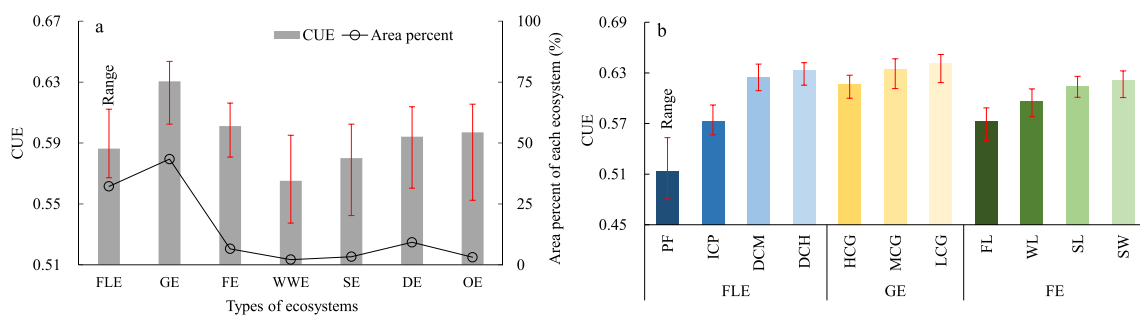


Fig. 3. Characteristics of CUE in different ecosystems (a) and their next level land use types (b). FLE: farmland ecosystem; GE: grassland ecosystem; FE: forest ecosystem; WWE: water and wetland ecosystem; SE: settlement ecosystem; DE: desert ecosystem; OE: other ecosystem; PF: paddy field; ICP: irrigated cropland on plain; DCM: dry cropland on mountain; DCH: dry cropland on hill; HCG: high coverage grassland; MCG: medium coverage grassland; LCG: low coverage grassland; FL: forest land; WL: woodland; SL: shrub land; SW: sparsely woodland.

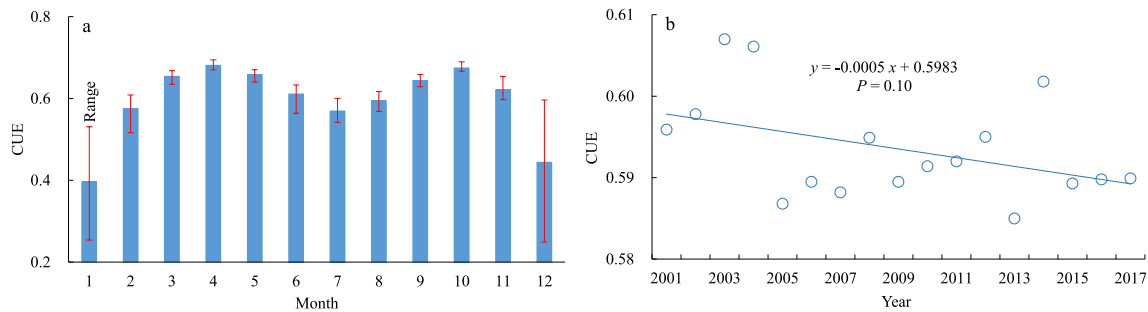


Fig. 4. Change of monthly CUE in a year (a) and trend of annual CUE from 2000 to 2017 (b).

phenomenon is a basic characteristic of plant growth in temperate zone. Meanwhile, the CUE in winter is lower but with a large variation since the data varies in annual cycle and the plant dormant in this season.

The annual CUE from each pixel in all ecosystem in Ningxia province was summarized and the linear trend of annual CUE from 2001 to 2017 is shown in Fig. 4b. The CUE had a slightly decreasing trend with the slope of 0.0005, which is meaningful although the  $p$ -value only is 0.10 (Bangdiwala, 2016). The results indicated that the efficiency of carbon uptake in Ningxia province decreased during the past 17 years and the potential of the carbon sequestration would reduce if the gross primary productivity was stable. The decreasing trend of CUE could be caused by the land use change of Ningxia province motivated by the vegetation restoration program. Since 1999, the Returning Farmland to Forest Program (RFFP; also translated as Sloping Land Conversion Program or Grain for Green Program) has been implemented in Ningxia province (Liu et al., 2008; Zinda et al., 2017). RFFP encouraged rural households to plant trees on marginal cropland or give up cultivating their dry cropland on mountains or hills for a natural grass restoration. As a result, a large amount of cultivated dry cropland has been turned into grassland, woodland or shrub land. As shown in Fig. 3b, these conversion could lead to the decreasing of CUE in the whole Ningxia province (Fig. 4b).

### 3.4. Variation of CUE at pixel scale

The linear trend of CUE at pixel scale that was calculated in IDL software using linear regression trend analysis was shown in Fig. 5a. There are 90.32% of whole area of Ningxia province with a negative slope of CUE in the period of 2001–2017, which indicated the efficiency of carbon uptake was decreasing in most regions. Nevertheless, the area with the linear slope range of  $-0.01$  to  $-0.02$  was  $3.24 \times 10^4 \text{ hm}^2$ , accounting for only 0.63% of the whole area of Ningxia province. An  $F$  test ( $P = 0.05$ ) was used to find the significance of the linear regression trend and its result shown in Fig. 5b. Although most pixels had a negative slope of CUE, the significantly decreasing area ( $P < 0.05$ ) was  $92.25 \times 10^4 \text{ hm}^2$  that accounted for 17.81% of whole area of Ningxia province. The Yellow River irrigation area of northern Ningxia, except for settlement ecosystem and the pumping irrigation area in arid zone of middle Ningxia, is the most significant area with decreasing CUE, where is usually found of low annual CUE value (Fig. 2) with paddy field and irrigated cropland in plain. In addition, some part of mountainous area of southern Ningxia also had a significant decreasing trend. In contrast, the significantly increasing area ( $P < 0.05$ ) were mostly located in arid zone of middle Ningxia, where one can find desert steppe, a typical grassland ecosystem in desert/grassland biome transition zone (with the linear slope of CUE in the range of  $0-0.01$ ). The significant increasing CUE area only accounted for 9.06% of whole area of Ningxia province. There are 73.13% of pixels in Ningxia province did not pass the  $F$  test ( $P = 0.05$ ) and their change trend is non-significant.

Under the current change trends of CUE, we used the rescaled range analysis to detect their characteristics of long-term persistence. Fig. 5c shows the Hurst exponent in map, the pixels with  $0.5 < H < 1$  and  $0 < H < 0.5$  were labeled as ‘persistent’ and ‘anti-persistent’ correspondingly.

There are 63.45% of pixels with the long-term persistent characteristics that would continue to maintain the original trend of change, while the 34.19% of pixels having the anti-persistent characteristics that would reverse their original trend of change. Combining the previous linear change trends, the future change trend map of CUE was derived (Fig. 5d). In total, 56.28% of Ningxia province will have a persistent CUE decreasing in future. The persistent CUE decreasing area are mainly located in irrigation area that include gravity irrigation area in Yellow River valley and pumping irrigation area in its branches with mainly farmland ecosystems. Furthermore, in the mountains and hills in southern Ningxia the CUE would persistently decrease in future in dry cropland of farmland ecosystem or medium to high coverage grassland ecosystem. Nevertheless, the CUE in 7.16% of whole province would increase persistently in future, where one can find desert steppe area located in the middle Ningxia.

### 3.5. Driving factors of CUE in the whole study area

#### 3.5.1. Variation of CUE in response to climate factors

The Ningxia province belongs to typical arid and semi-arid climate that has obvious seasonal changes during the year including periodic precipitation and temperature variation. The rainy season came with the rising of air temperature (Fig. 6a,b) that induced a seasonal phenology of plant in this area. Here, we used a method of partial correlation under the controlling variable of GPP to find the relationship between CUE and climatic factors. In January and December, the coldest month of a year, the photosynthesis of plant is very weak due to low air temperatures and dormancy of plant. Thus, the GPP of ecosystem is low and the CUE is not only low but also with a lot of noise (Fig. 4a). As a consequence, the monthly data from 2001 to 2017 except January and December was used for the partial correlation analysis. Fig. 6c showed that the precipitation had a negative correlation with the CUE under the controlling variable of GPP. The significant partial correlation coefficient was  $-0.26$  ( $P < 0.01$ ) that indicated the CUE would decrease with the rising of precipitation under the condition that the controlled GPP of ecosystem did not fluctuate with the phenology of plant. However, the temperature had a positive correlation with the CUE under the controlling variable of GPP (Fig. 6d), in opposite to precipitation. Although there was a lower partial correlation coefficient ( $R = -0.16$ ,  $P < 0.05$ ), it indicated the rising of air temperature could enhance the CUE of ecosystem that would promote the ecosystem transferring more carbon from atmosphere in Ningxia province under the global warming background. This positive temperature-CUE relation implies that the ecosystem could have stronger ability on accumulating NPP when they are under the drought stress (low precipitation and high air temperature).

#### 3.5.2. Variation of CUE in response to ecosystem processes

Driven by the temperate continental climate, the plant growth in Ningxia province has a particular plant phenology. Most species sprouted early in March and became thoroughly dormant till November and, correspondingly, the GPP, NPP and autotrophic respiration consumption changed with this rhythm and their profiles had similar shapes with

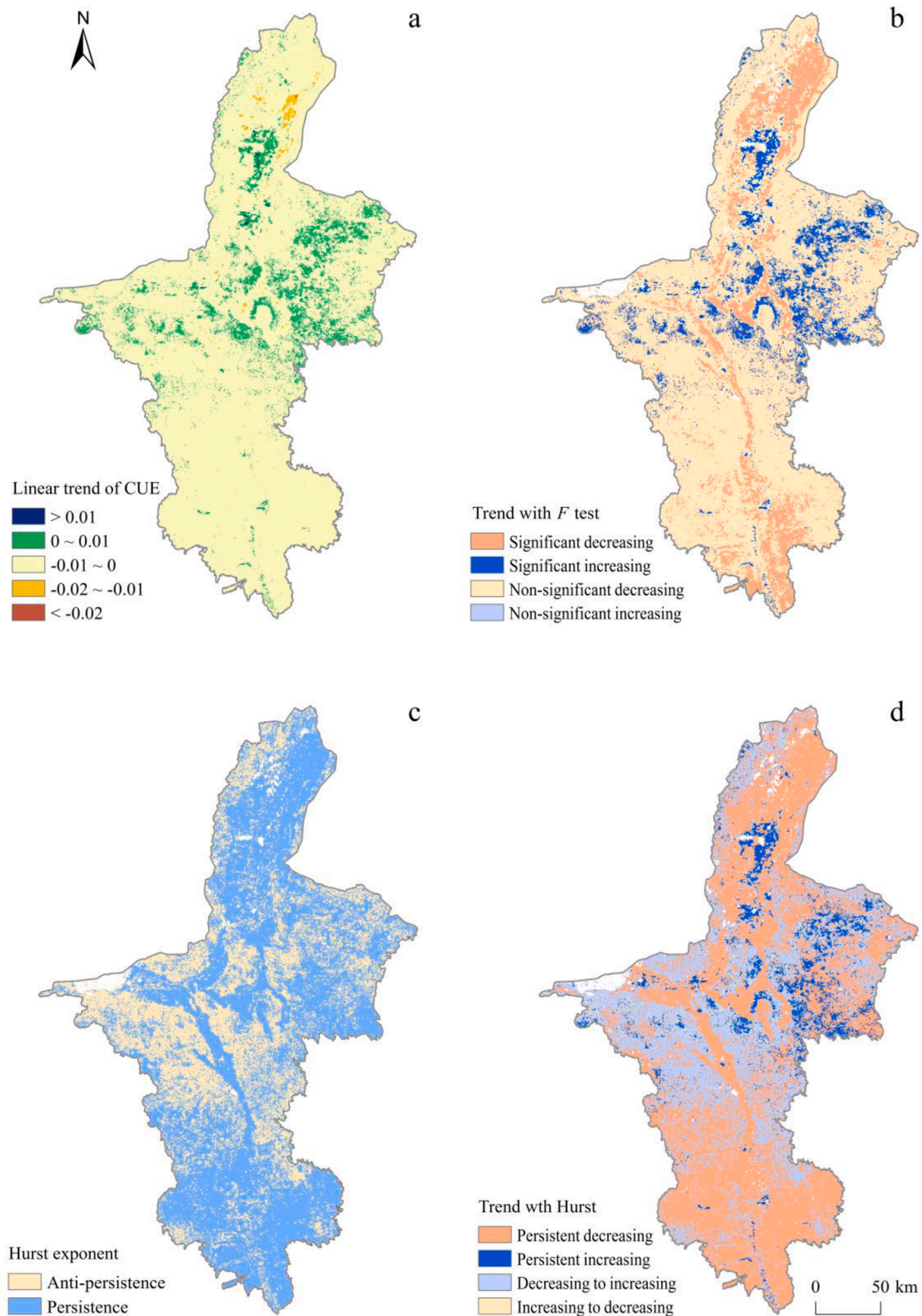


Fig. 5. Linear trend, significance test, Hurst exponent and sustainability map of CUE.

single peaks although they did not appear in the same month (Fig. 7a). The amount of carbon entering the ecosystems and the organic matter consumption supporting daily ecosystem processes can be described by NPP and  $R_a$ . Thus, the NPP and  $R_a$  were used to analyze the variation of CUE in response to ecosystem processes. Because GPP represents growth

activities of plant, we used GPP as the controlling variable to carry out partial correlation analysis between CUE and  $R_a$ . As shown in Fig. 7b, the CUE had a strong negative correlation with  $R_a$  with a coefficient of  $-0.79$  ( $P < 0.01$ ). But the scatter plot had sparse dots with the increasing of  $R_a$ . The result revealed that the ecosystem would decrease their capability to

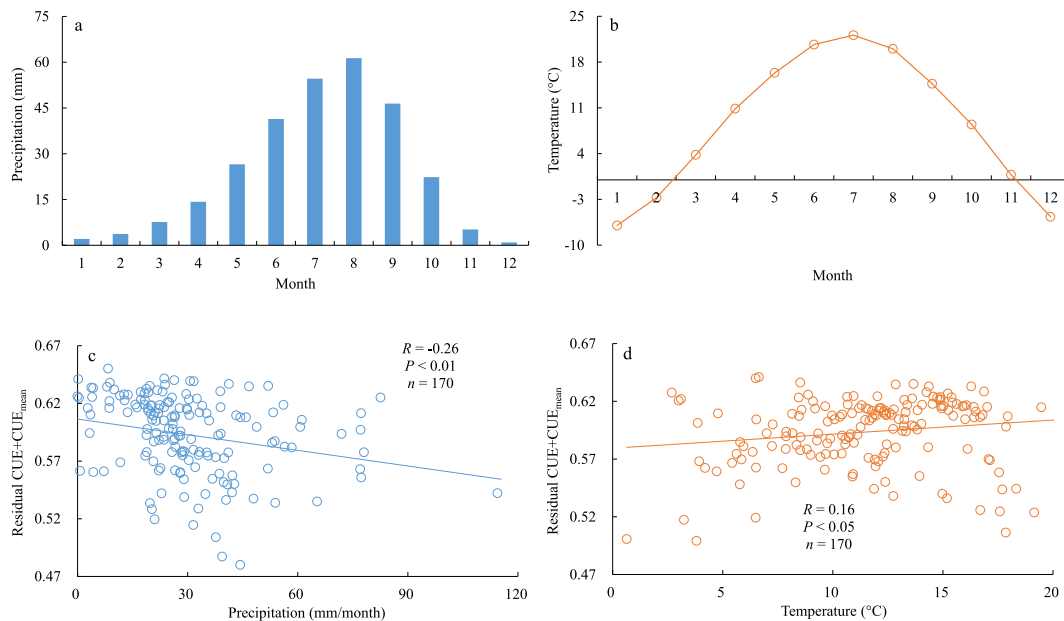


Fig. 6. Monthly precipitation (a) and temperature (b) in a year and partial correlation between temperature (c), precipitation (d) and CUE in Ningxia.

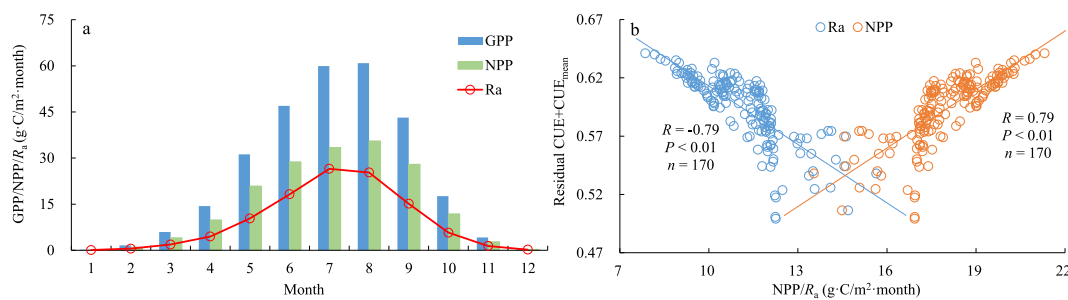


Fig. 7. Monthly GPP, NPP and  $R_a$  and partial correlation between CUE and NPP/ $R_a$  in Ningxia.

capture carbon from atmosphere with the increasing of  $R_a$ . The NPP had a positive correlation with the CUE under the controlling variable of GPP that was completely opposite with the  $R_a$  (see Eq. (1)).

### 3.6. Driving factors of CUE in various ecosystems

For the seven ecosystems described in Section 1.3, the partial correlation analysis between CUE and precipitation, temperature, NPP,  $R_a$  was analyzed for each ecosystem respectively. As shown in Fig. 8, the precipitation had the same negative correlation with CUE for all ecosystems with high level of significance ( $P < 0.01$ ) ranging from  $-0.20$  to  $-0.30$ . However, air temperature that had a variable correlation with CUE at different ecosystems across the whole Ningxia province. The farmland ecosystem (FLE), forest ecosystem (FE) and the settlement ecosystem (SE) had negative correlation between air temperature and CUE with a significance of  $P < 0.01$  or  $P < 0.05$ . The grassland ecosystem (GE) and water and wetland ecosystem (WWE) had no significant correlation between air temperature and CUE since they had a much lower  $P$  value. On the contrast, CUE of desert ecosystem (DE) and other ecosystem (OE) had a significant positive correlation with air temperature ( $P < 0.01$ ), although their area only accounted for 9.25% and 3.10% of the whole Ningxia province respectively.

The indices for ecosystem process such as NPP and  $R_a$  were also significantly correlated with the CUE of each ecosystems (Fig. 8). The NPP had a positive correlation with the CUE under the controlling variable of GPP and the partial correlation coefficients ranged from 0.78 to 0.89 in different ecosystems. The ranges of NPP differ in different

ecosystems with the corresponding different ranges of GPP. For example, the farmland ecosystem and forest ecosystem had higher NPP, while the desert ecosystem and other ecosystem had lower NPP. Nevertheless, autotrophic respiration consumption was negatively correlated with the CUE in seven ecosystems consistently. Their partial correlation coefficients ranged from  $-0.78$  to  $-0.89$  and all passed the significance test ( $P < 0.01$ ).

## 4. Discussion

### 4.1. Precision of CUE based on MODIS data

The CUE of terrestrial ecosystem is defined as the ratio of NPP to GPP as an accepted practice. However, the NPP and GPP estimated by different methods could cause the CUE values varying in a large range. Most studies of plant physiology found that CUE was around 0.5 and this value was defined as a constant value in many physiological and ecological models. A NPP/GPP ratio of  $0.47 \pm 0.04$  (SD) was first suggested for forest as universal across biomes, tree species and stand ages (Waring et al., 1998). But later studies reported substantial variation in CUE in different forest types, which make the hypothesis of constant CUE invalid (Delucia et al., 2007). In addition, the fertilization or irrigation could alter the ratio of NPP and  $R_a$  in some species with the increasing GPP. A survey over 200 studies showed that the average NPP/GPP ratio from different biomes, species and forest stand ages should be 0.46, but with a large variation range (0.22–0.79) (Collalti and Prentice, 2019). Here, we obtained the average annual CUE from MODIS data that



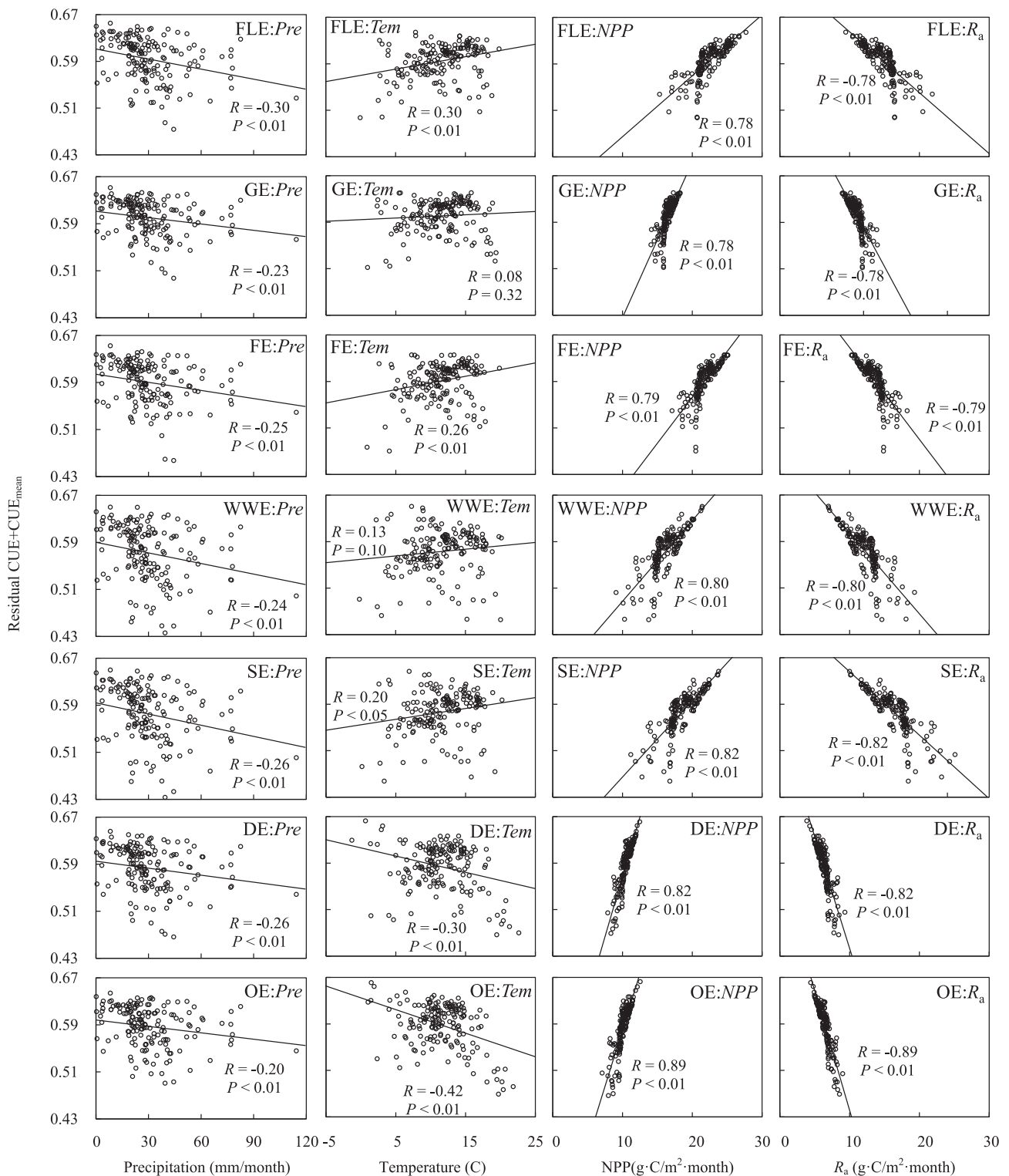


Fig. 8. Partial correlation scatter plots between precipitation, temperature, NPP, R<sub>a</sub> and CUE in various ecosystems. Note: abbreviation as show in Fig. 3.

has an average value of 0.59 although it varies with ecosystem types. By comparison with literature data mentioned above the MODIS CUE is higher than their average but still falls in the scatter area of previous studies (Fig. 9). The CUE range of 0.57–0.63 in seven ecosystems of Ningxia province has an acceptable precision for our purpose, especially because we pay more attention on the spatio-temporal changes of CUE as relative variation. Nevertheless, the MODIS NPP and GPP of the low biomass ecosystems in desert/grassland biome transition zone with the

arid and semi-arid environment are lower than measured ones from literature (Fig. 9 have different X, Y axis). The coarse resolution of the spatially observed data from MODIS with 500 m resolution also causes lower NPP and GPP than those measured from a certain tree species. The mixed pixel of a heterogeneous land surface could cover various ecosystem types, which is not only the barrier to calculate the CUE accurately in this research but also is one of the biggest challenges of remote sensing applications in most fields.

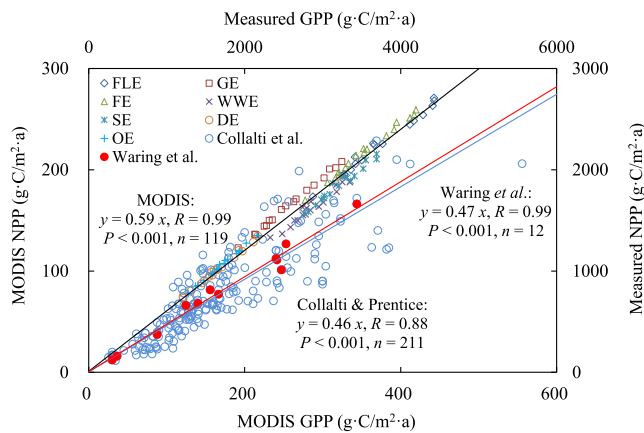


Fig. 9. Comparison of NPP: GPP (CUE) between MODIS and literature survey. Note: abbreviation as show in Fig. 3.

#### 4.2. Driving mechanism of CUE variation

The partial correlation analysis results showed that the CUE depends on the main climatic characteristics such as temperature and precipitation. The results suggested that the ecosystem could uptake more carbon from the atmosphere with the same GPP level when it is under the drought stress (low precipitation and high air temperature). Nevertheless, the mechanism of climate driven CUE variation is not yet fully understood. Even though higher CO<sub>2</sub> concentrations in future decades can increase GPP, the climate change induced drought, e.g. low soil water availability and heat stress, could reduce GPP at the same time (Xu et al., 2019). The heat and drought in 2003 had caused a 30% reduction in GPP over Europe, which resulted in a strong anomalous carbon cycle, but ecosystem respiration decreased with GPP, rather than accelerating with the temperature rise in the European drought event (Ciais et al., 2005). The unusual response of ecosystem to drought was also detected in Amazonia during the strong drought in 2010, when the GPP was suppressed while the NPP remained constant throughout the drought and autotrophic respiration decreased extensively, especially at the end of the drought (Doughty et al., 2015). Thus, we can conclude that the variability of GPP, NPP and R<sub>a</sub> induced the increased CUE with the drought stress (low precipitation and high air temperature) during the dry period of whole Ningxia province (Du et al., 2015) (see Section 2.5.1). The smart plants could increase their efficiency of transforming carbon from the atmosphere to terrestrial biomass in adverse environment, especially in the arid and semi-arid region. Nevertheless, the mechanism of climate driven CUE variation at ecosystem scale was inconsistent with that at regional scale, which should be studied further. And, the land use change caused by anthropogenic activities, e.g. RFPF, is one of driving forces for CUE variations, which should be also investigated in future studies.

#### 4.3. Limitation of remote sensing and meteorological data

The temporal characteristics of CUE were limited by the temporal length of MODIS time series data, because the statistical trends and Hurst phenomenon are based on a statistical theory over a large sample size. Even though the monthly CUE data from 2001 to 2017 is almost the longest period after the MODIS launch, there are some pixels did not pass the significance test. Meanwhile, the other challenge comes from the algorithm of MOD17A2 since it has an underestimation of GPP in the dry area (Sjöström et al., 2013). The MOD17A2 GPP is derived from the MOD15A2 LAI/FPAR, but the algorithm of MOD15A2 has a challenge in farmland since it can not appropriately simulate the swift change of the phenological phase at harvest. Although the normalized difference vegetation index (NDVI) was used to estimate the LAI/FPAR in the backup algorithm that will partially eliminate the effect of crop phenology on the

estimation of LAI/FPAR and GPP, it still needs to make an improvement by the algorithm scientist in the future. Finally, the meteorological data used in this study is sparse, since there are only 10 stations in the area of  $5.18 \times 10^6$  hm<sup>2</sup> with heterogeneous land surface. Therefore, the average value of climate factor was used to perform partial correlation analysis with CUE rather than the gridded climate data. Climate data with 500 m resolution is still an obstacle for this purpose. However, the recently published high-resolution meteorological dataset (He et al., 2020) will take a new chance for our work.

## 5. Conclusions

Based on the CUE of terrestrial ecosystem estimated by MODIS data from 2001 to 2017, the spatial and temporal characteristics of CUE in Ningxia province, a typical desert/grassland biome transition zone, were studied and the main driving factors were revealed. The following conclusions are obtained: (1) The CUE of terrestrial ecosystems in desert/grassland biome transition zone is higher than the CUE of 0.5 defined in many ecological models and varied with the ecosystem types even when they are located in the same climatic zone. (2) The bad habitat condition (e.g. lower canopy density, water stress) in a certain ecosystem could increase its CUE, which indicates the smart strategy of plants to increase their efficiency of transforming carbon from the atmosphere to terrestrial biomass in adverse environment. (3) The CUE significantly responds to NPP and R<sub>a</sub> at the same GPP level, meanwhile lower precipitation and higher temperature associated with drought could increase the CUE in desert/grassland biome transition zone.

#### CRedit authorship contribution statement

**Lingtong Du:** Conceptualization, Methodology, Writing - review & editing. **Fei Gong:** Software, Writing - original draft. **Yijian Zeng:** Writing - review & editing. **Longlong Ma:** Formal analysis. **Chenglong Qiao:** Data collection. **Hongyue Wu:** Visualization.

#### Declaration of Competing Interest

The authors declare that they have no known competing financial interests or personal relationships that could have appeared to influence the work reported in this paper.

#### Acknowledgements

This work was supported by the National Science Foundation of China (No. 41967027, 41661003), the Ningxia Excellent Talents Support Program (No. RQ0012) and the First Class Disciplines Program of Ningxia Province (No. NXYLXK2017B06). We appreciate the United States Geological Survey, China Meteorological Administration and Cold and Arid Regions Science Data Center at Lanzhou for sharing datasets. We are also grateful to Pro. Dr. Z. Su, ITC of University of Twente, for his valuable comments and checking the English in our paper.

#### References

- Araujo, M.V.O., Celeste, A.B., 2019. Rescaled range analysis of streamflow records in the São Francisco River Basin, Brazil. *Theor. Appl. Climatol.* 135, 249–260.
- Baba, K., Shibata, R., Sibuya, M., 2004. Partial correlation and conditional correlation as measures of conditional independence. *Aust. N. Z. J. Stat.* 46, 657–664.
- Baldocchi, D.D., Hincks, B.B., Meyers, T.P., 1988. Measuring biosphere-atmosphere exchanges of biologically related gases with micrometeorological methods. *Ecology* 69, 1331–1340.
- Bangdiwala, S.I., 2016. Understanding significance and p-values. *Nepal J. Epidemiol.* 6, 522–524.
- Bastin, J.-F., Finegold, Y., Garcia, C., Mollicone, D., Rezende, M., Routh, D., Zohner, C. M., Crowther, T.W., 2019. The global tree restoration potential. *Science* 365, 76–79.
- Chambers, J.Q., Tribuzy, E.S., Toledo, L.C., Crispim, B.F., Higuchi, N., Santos, J.D., Araújo, A.C., Kruijt, B., Nobre, A.D., Trumbore, S.E., 2004. Respiration from a tropical forest ecosystem: Partitioning of sources and low carbon use efficiency. *Ecol. Appl.* 14, 72–88.

- Chen, C., Park, T., Wang, X., Piao, S., Xu, B., Chaturvedi, R.K., Fuchs, R., Brovkin, V., Ciais, P., Fensholt, R., Tømmervik, H., Bala, G., Zhu, Z., Nemani, R.R., Myneni, R.B., 2019. China and India lead in greening of the world through land-use management. *Nat. Sustain.* 2, 122–129.
- Choudhury, B.J., 2000. Carbon use efficiency, and net primary productivity of terrestrial vegetation. *Adv. Space Res.* 26, 1105–1108.
- Ciais, P., Reichstein, M., Viovy, N., Granier, A., Ogee, J., Allard, V., Aubinet, M., Buchmann, N., Bernhofer, C., Carrara, A., Chevallier, F., De Noblet, N., Friend, A.D., Friedlingstein, P., Grünwald, T., Heinesch, B., Keronen, P., Knohl, A., Krinner, G., Loustau, D., Manca, G., Matteucci, G., Miglietta, F., Ourcival, J.M., Papale, D., Pilegaard, K., Rambal, S., Seufert, G., Soussana, J.F., Sanz, M.J., Schulze, E.D., Vesala, T., Valentini, R., 2005. Europe-wide reduction in primary productivity caused by the heat and drought in 2003. *Nature* 437, 529–533.
- Collalti, A., Prentice, I.C., 2019. Is NPP proportional to GPP? Waring's hypothesis 20 years on. *Tree Physiol.* 39, 1473–1483.
- Curtis, P., Vogel, C., Gough, C., Schmid, H., Su, H.B., Bovard, B., 2005. Respiratory carbon losses and the carbon-use efficiency of a northern hardwood forest, 1999–2003. *New Phytol.* 167, 437–456.
- Delucia, E.H., Drake, J.E., Thomas, R.B., Gonzalez-Meler, M., 2007. Forest carbon use efficiency: Is respiration a constant fraction of gross primary production? *Glob. Change Biol.* 13, 1157–1167.
- Dillaway, D.N., Kruger, E.L., 2014. Trends in seedling growth and carbon-use efficiency vary among broadleaf tree species along a latitudinal transect in eastern North America. *Glob. Change Biol.* 20, 908–922.
- Doughty, C.E., Metcalfe, D.B., Girardin, C.A.J., Amézquita, F.F., Cabrera, D.G., Huasco, W. H., Silva-Espejo, J.E., Araujo-Murakami, A., da Costa, M.C., Rocha, W., Feldpausch, T. R., Mendoza, A.L.M., da Costa, A.C.L., Meir, P., Phillips, O.L., Malhi, Y., 2015. Drought impact on forest carbon dynamics and fluxes in Amazonia. *Nature* 519, 78–82.
- Du, L., Song, N., Liu, K., Hou, J., Hu, Y., Zhu, Y., Wang, X., Wang, L., Guo, Y., 2017. Comparison of two simulation methods of the temperature vegetation dryness index (TVDI) for drought monitoring in semi-arid regions of China. *Remote Sens.* 9, 177.
- Du, L., Song, N., Wang, L., Nan, L., 2015. Characteristics of drought variations in Ningxia from 1960 to 2012 under background of climate change. *J. Nat. Disasters* 24, 157–164 (in Chinese with an English abstract).
- Du, L., Tian, Q., Yu, T., Meng, Q., Jancso, T., Urdvardy, P., Huang, Y., 2013. A comprehensive drought monitoring method integrating MODIS and TRMM data. *Int. J. Appl. Earth Obs. Geoinf.* 23, 245–253.
- Erb, K.-H., Kastner, T., Plutzer, C., Bais, A.L.S., Carvalhais, N., Fetzel, T., Gingrich, S., Haberl, H., Lauk, C., Niedertscheider, M., 2018. Unexpectedly large impact of forest management and grazing on global vegetation biomass. *Nature* 553, 73–76.
- Falkowski, P., Scholes, R., Boyle, E., Canadell, J., Canfield, D., Elser, J., Gruber, N., Hibbard, K., Höglberg, P., Linder, S., 2000. The global carbon cycle: a test of our knowledge of earth as a system. *Science* 290, 291–296.
- Fang, J., Yu, G., Liu, L., Hu, S., Chapin, F.S., 2018. Climate change, human impacts, and carbon sequestration in China. *Proc. Natl. Acad. Sci. USA* 115, 4015–4020.
- Fay, P.A., Kaufman, D.M., Nippert, J.B., Carlisle, J.D., Harper, C.W., 2008. Changes in grassland ecosystem function due to extreme rainfall events: Implications for responses to climate change. *Glob. Change Biol.* 14, 1600–1608.
- Feng, X.M., Fu, B.J., Piao, S., Wang, S.H., Ciais, P., Zeng, Z.Z., Lu, Y.H., Zeng, Y., Li, Y., Jiang, X.H., Wu, B.F., 2016. Revegetation in China's Loess Plateau is approaching sustainable water resource limits. *Nat. Clim. Chang.* 6, 1019–1022.
- Gang, C., Wang, Z., Chen, Y., Yang, Y., Li, J., Cheng, J., Qi, J., Odeh, I., 2016. Drought-induced dynamics of carbon and water use efficiency of global grasslands from 2000 to 2011. *Ecol. Indic.* 67, 788–797.
- Gebremichael, M., Barros, A.P., 2006. Evaluation of MODIS Gross Primary Productivity (GPP) in tropical monsoon regions. *Remote Sens. Environ.* 100, 150–166.
- Ghulam, A., Qin, Q., Teyip, T., Li, Z.-L., 2007. Modified perpendicular drought index (MPDI): A real-time drought monitoring method. *ISPRS-J. Photogramm. Remote Sens.* 62, 150–164.
- He, J., Yang, K., Tang, W., Lu, H., Qin, J., Chen, Y., Li, X., 2020. The first high-resolution meteorological forcing dataset for land process studies over China. *Sci. Data* 7, 25.
- He, Y., Piao, S., Li, X., Chen, A., Qin, D., 2018. Global patterns of vegetation carbon use efficiency and their climate drivers deduced from MODIS satellite data and process-based models. *Agric. For. Meteorol.* 256, 150–158.
- Ho, P., 2000. The myth of desertification at China's northwestern frontier: the case of Ningxia Province, 1929–1958. *Mod. China* 26, 348–395.
- Hou, G., Sun, J., Wang, J., 2018. Dynamics and controls of carbon use efficiency across China's grasslands. *Pol. J. Environ. Stud.* 27, 1541–1550.
- Hou, J., Du, L., Liu, K., Hu, Y., Zhu, Y., 2019. Characteristics of vegetation activity and its responses to climate change in desert/grassland biome transition zones in the last 30 years based on GIMMS3g. *Theor. Appl. Climatol.* 136, 915–928.
- Keenan, T.F., Hollinger, D.Y., Bohrer, G., Dragoni, D., Munger, J.W., Schmid, H.P., Richardson, A.D., 2013. Increase in forest water-use efficiency as atmospheric carbon dioxide concentrations rise. *Nature* 499, 324–327.
- Kwon, Y., Larsen, C.P., 2013. Effects of forest type and environmental factors on forest carbon use efficiency assessed using MODIS and FIA data across the eastern USA. *Int. J. Remote Sens.* 34, 8425–8448.
- Letchov, G., 2018. Carbon-use efficiency of terrestrial ecosystems under stress conditions in South East Europe (MODIS, NASA). *Proceedings* 2, 363.
- Li, S.S., Yan, J.P., Liu, X.Y., Wan, J., 2013. Response of vegetation restoration to climate change and human activities in Shaanxi-Gansu-Ningxia Region. *J. Geogr. Sci.* 23, 98–112.
- Liu, J., Li, S., Ouyang, Z., Tam, C., Chen, X., 2008. Ecological and socioeconomic effects of China's policies for ecosystem services. *Proc. Natl. Acad. Sci. USA* 105, 9477–9482.
- Lu, F., Hu, H., Sun, W., Zhu, J., Liu, G., Zhou, W., Zhang, Q., Shi, P., Liu, X., Wu, X., 2018. Effects of national ecological restoration projects on carbon sequestration in China from 2001 to 2010. *Proc. Natl. Acad. Sci. USA* 115, 4039–4044.
- Manzoni, S., Capek, P., Porada, P., Thurner, M., Winterdahl, M., Beer, C., Bruchert, V., Frouz, J., Herrmann, A.M., Lindahl, B.D., 2018. Reviews and syntheses: Carbon use efficiency from organisms to ecosystems – Definitions, theories, and empirical evidence. *Biogeosciences* 15, 5929–5949.
- Moya-Laraño, J., Corcobado, G., 2008. Plotting partial correlation and regression in ecological studies. *Web Ecol.* 8, 35–46.
- Ogawa, K., 2011. Theoretical analysis of change in forest carbon use efficiency with stand development: A case study on Hinoki Cypress (*Chamaecyparis obtusa* (Sieb. et Zucc.) Endl.) plantation from the seedling stage. *Ecol. Model.* 222, 437–441.
- Ouyang, Z., Zhang, L., Wu, B., Li, X., Xu, W., Xiao, Y., Zheng, H., 2015. An ecosystem classification system based on remote sensor information in China. *Acta Ecol. Sin.* 35, 219–226 (in Chinese with an English abstract).
- Piao, S., Luysaert, S., Ciais, P., Janssens, I.A., Chen, A., Cao, C., Fang, J., Friedlingstein, P., Luo, Y., Wang, S., 2010. Forest annual carbon cost: A global-scale analysis of autotrophic respiration. *Ecology* 91, 652–661.
- Poulter, B., Frank, D., Ciais, P., Myneni, R.B., Andela, N., Bi, J., Broquet, G., Canadell, J. G., Chevallier, F., Liu, Y.Y., Running, S.W., Sitch, S., van der Werf, G.R., 2014. Contribution of semi-arid ecosystems to interannual variability of the global carbon cycle. *Nature* 509, 600–603.
- Rodionov, A., Amelung, W., Peinemann, N., Haumaier, L., Zhang, X., Kleber, M., Glaser, B., Urusevskaya, I., Zech, W., 2010. Black carbon in grassland ecosystems of the world. *Glob. Biogeochem. Cycle* 24, GB3013.
- Running, S.W., Nemani, R.R., Heinsch, F.A., Zhao, M., Reeves, M., Hashimoto, H., 2004. A continuous satellite-derived measure of global terrestrial primary production. *Bioscience* 54, 547–560.
- Running, S.W., Zhao, M., 2015. Daily GPP and annual NPP (MOD17A2/A3) products NASA Earth Observing System MODIS land algorithm. MOD17 User's Guide 2015.
- Schimel, D., Pavlick, R., Fisher, J.B., Asner, G.P., Saatchi, S., Townsend, P., Miller, C., Frankenberg, C., Hibbard, K., Cox, P., 2015. Observing terrestrial ecosystems and the carbon cycle from space. *Glob. Change Biol.* 21, 1762–1776.
- Schimel, D.S., 1995. Terrestrial ecosystems and the carbon cycle. *Glob. Change Biol.* 1, 77–91.
- Scurlock, J., Hall, D., 1998. The global carbon sink: A grassland perspective. *Glob. Change Biol.* 4, 229–233.
- Sjöström, M., Ardö, J., Arneth, A., Boulain, N., Cappelare, B., Eklundh, L., de Grandcourt, A., Kutsch, W.L., Merbold, L., Nouvellon, Y., Scholes, R.J., Schubert, P., Seaquist, J., Veenendaal, E.M., 2011. Exploring the potential of MODIS EVI for modeling gross primary production across African ecosystems. *Remote Sens. Environ.* 115, 1081–1089.
- Sjöström, M., Ardö, J., Eklundh, L., El-Tahir, B.A., El-Khidir, H.A.M., Hellström, M., Pilesjö, P., Seaquist, J., 2009. Evaluation of satellite based indices for gross primary production estimates in a sparse savanna in the Sudan. *Biogeosciences* 6, 129–138.
- Sjöström, M., Zhao, M., Archibald, S., Arneth, A., Cappelare, B., Falk, U., de Grandcourt, A., Hanan, N., Kergoat, L., Kutsch, W., Merbold, L., Mougou, E., Nickless, A., Nouvellon, Y., Scholes, R.J., Veenendaal, E.M., Ardö, J., 2013. Evaluation of MODIS gross primary productivity for Africa using eddy covariance data. *Remote Sens. Environ.* 131, 275–286.
- Tian, X., Xue, X., Liao, J., Du, H., Duan, H., Xu, M., 2014. Land use change in the watershed of the Ningxia-Inner Mongolia reaches of the Yellow River during 1990–2010. *J. Desert Res.* 34, 1167–1176 (in Chinese with an English abstract).
- Wang, Y., Gao, J., Wang, J., Qiu, J., 2014. Value assessment of ecosystem services in nature reserves in Ningxia, China: a response to ecological restoration. *PLoS One* 9, e89174.
- Waring, R., Landsberg, J., Williams, M., 1998. Net primary production of forests: A constant fraction of gross primary production? *Tree Physiol.* 18, 129–134.
- Xu, C., McDowell, N.G., Fisher, R.A., Wei, L., Sevanto, S., Christoffersen, B.O., Weng, E., Middleton, R.S., 2019. Increasing impacts of extreme droughts on vegetation productivity under climate change. *Nat. Clim. Chang.* 9, 948–953.
- Yang, Y., Wang, Z., Li, J., Gang, C., Zhang, Y., Odeh, I., Qi, J., 2017. Assessing the spatiotemporal dynamic of global grassland carbon use efficiency in response to climate change from 2000 to 2013. *Acta Oecol.-Int. J. Ecol.* 81, 22–31.
- Zhang, Y., Xu, M., Chen, H., Adams, J., 2009. Global pattern of NPP to GPP ratio derived from MODIS data: effects of ecosystem type, geographical location and climate. *Glob. Ecol. Biogeogr.* 18, 280–290.
- Zhao, M., Running, S.W., 2010. Drought-induced reduction in global terrestrial net primary production from 2000 through 2009. *Science* 329, 940–943.
- Zinda, J.A., Trac, C.J., Zhai, D., Harrell, S., 2017. Dual-function forests in the returning farmland to forest program and the flexibility of environmental policy in China. *Geoforum* 78, 119–132.